

# Control of Ring OSF in Large Diameter Czochralski Silicon Crystals

Teruyuki TAMAKI<sup>1</sup>  
Kuniteru OTA<sup>2</sup>

Katsuhiko NAKAI<sup>1</sup>  
Wataru OHASHI<sup>1</sup>

## Abstract

*There is a vacancy dominant region in the crystal center of the silicon crystals and an interstitial atom dominant region in the peripheral area when the crystal growth rate is within a certain range, and ring OSFs form near the boundary of the two. To obtain good quality wafers it is important to control the ring OSFs, and this is one of the problems to overcome for the production of large diameter silicon crystals or the quality enhancement of epitaxial wafers using high-dope crystal substrates. This report experimentally clarifies the formation mechanisms of the ring OSFs and shows that the mechanisms can be described by expanding an easy one-dimension model to two dimensions. The ring OSFs appear when the crystal growth rate and the temperature gradient in the crystal growth direction are in a certain ratio to each other. Further, in the case of boron high dope crystals, the ring OSFs form when the ratio is comparatively high, which fact can be explained by factors such as the decrease in mobility of vacancies. It is expected that a quality design based on these findings will make the production of large diameter and high quality crystals possible.*

## 1. Introduction

Recent trends of higher integration and a finer design rule of silicon devices demand expansion of silicon crystal diameter and enhancement of crystal quality. The expansion of crystal diameter envisages minimizing the increase in the device manufacturing cost in increasing the chip size. Most of the silicon wafers for LSIs nowadays are grown using the Czochralski process. The dominant diameter of the wafers is 200 mm at present, but device makers plan to introduce 300-mm diameter wafers from 2001.

The silicon crystals by the Czochralski process (CZ-Si) contain grown-in defects (void defects<sup>1)</sup> and dislocation cluster defects<sup>2)</sup> introduced during the crystal growth, and their type and characteristic depend largely on the crystal's condition at the solid/liquid boundary and thermal history at high temperatures. Crystal properties along a radial direction of a 300-mm diameter crystal tend to be less homo-

geneous than those of a crystal 200 mm or less in diameter. This is because the condition at the solid/liquid boundary and the thermal history at high temperatures differ more widely along crystal radius as the diameter increases.

Nippon Steel has clarified defect formation mechanisms and developed defect control measures based on the clarified mechanisms aiming at expanding the crystal diameter and enhancing the crystal quality through epitaxial wafers using high-dope crystal substrates.

## 2. Relationship between Ring OSF and Crystal Growth Conditions

Usually, in the CZ-Si's, when they are grown at a certain pulling rate, there are regions of void defects, a kind of as-grown defect, near the center and regions of dislocation clusters defects near the

<sup>1</sup> Technical Development Bureau

<sup>2</sup> NIPPON STEEL TECHNORESEARCH CORPORATION

crystal edge. After an oxidation heat treatment at 1,100°C for 1 h, a ring-shaped oxidation-induced stacking fault (ring OSF) is formed near the boundary between the void defect region and the dislocation cluster defect region<sup>3</sup>. Whereas the void defects and the dislocation cluster defects are the defects existing in as-grown crystals, the ring OSF is latent in the as-grown crystals, though it has already been introduced, and becomes manifest during device manufacturing processes. Under a slow crystal growth rate the dislocation cluster defects spread over the entire wafer, whereas under a high crystal growth rate the void defects spread over the entire wafer. When the crystal growth rate is somewhere in the middle, the void defects appear in the crystal center, the dislocation cluster defects appear in the peripheral region, and the ring OSF around the boundary of the two. As the crystal growth rate increases, the ring OSF moves towards the wafer edge (see Fig. 1)<sup>4</sup>.

Expressing crystal growth rate as  $V$  and temperature gradient in the crystal growth direction at the crystal center as  $G_0$ , the ring OSF appears at the crystal center when the ratio  $V/G_0$  takes a critical value  $(V/G_0)_{crit}$ , and the radius of the ring OSF increases as  $V/G_0$  surpasses the critical value  $(V/G_0)_{crit}$ <sup>5</sup>. This is because the temperature gradient in the crystal growth direction  $G$  changes along a radius. Since the temperature gradient in the crystal growth direction  $G$  is larger near the crystal edge than near the center, the ring OSF radius is considered to increase as  $V/G_0$  becomes larger (see Fig. 2)<sup>6</sup>.

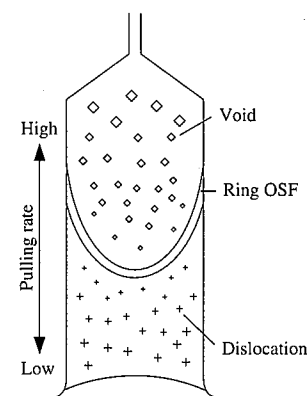


Fig. 1 Crystal growth rate and defect distribution

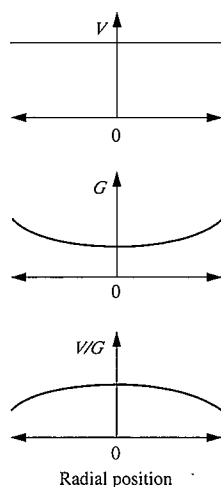


Fig. 2 Crystal growth rate and temperature gradient along crystal growth direction in crystal section

### 3. Ring OSF in Large Diameter, High-Dope Silicon Crystal

The relationship between the ring OSF radius and  $V/G(r)$  using crystals 300 mm in diameter was examined. Here,  $G(r)$  is temperature gradient in the crystal growth direction at a crystal radius  $r$ . Although control of the ring OSF is more difficult in the 300-mm diameter crystals, it is easier with large diameter crystals to accurately measure radial position dependency of the temperature gradient in the crystal growth direction.

Epitaxial wafers, which are not easily affected by grown-in defects, are expected to be dominant when the 300-mm diameter wafers become widely used. The epitaxial wafers are products of epitaxial layer growth of silicon on polished wafers made from CZ-Si. Here, P<sup>+</sup> substrates and P<sup>++</sup> substrates with a large addition of boron, a P type dopant, are used as the substrate polished wafers. Resistivity of a P<sup>+</sup> crystal is, normally, 10 to 20 m Ω·cm and that of a P<sup>++</sup> crystal is 5 to 10 m Ω·cm. In contrast, resistivity of a P<sup>-</sup> crystal, which is used as a polished wafer, is in the order of tens of Ω·cm. In terms of boron concentration, a P<sup>-</sup> crystal contains roughly 10<sup>14</sup> to 10<sup>15</sup> atoms/cm<sup>3</sup> of boron, and a P<sup>+</sup> crystal roughly 10<sup>18</sup> atoms/cm<sup>3</sup>.

Boron has been reported to affect distribution of the ring OSF in the CZ-Si crystals<sup>7</sup>. When CZ-Si's are grown under a common condition except for boron concentration, the ring OSF appears nearer to the crystal center as the boron concentration increases. This is accounted for by a decrease in mobility of vacancies in the crystal<sup>8</sup> as well as by a decrease in the concentration of supersaturated vacancies in the crystal<sup>9</sup>. Tests were conducted to quantitatively evaluate the effect of boron addition on the grown-in defects.

### 4. Test Method and Results

#### 4.1 Crystal growth

300-mm diameter silicon crystals were grown by the CZ process under the same hot-zone conditions (heat insulation structure). P<sup>-</sup> crystals and P<sup>+</sup> crystals were pulled up having boron concentration of 5.6 to 14.0 × 10<sup>14</sup> atoms/cm<sup>3</sup> and 4.7 to 10.4 × 10<sup>18</sup> atoms/cm<sup>3</sup>, respectively. Photo 1 shows one of the 300-mm diameter crystals thus pulled up and a 300-mm diameter wafer manufactured from it. In order to change the position of the ring OSF, different crystals were pulled up under different crystal growth rates as shown in Fig. 1.

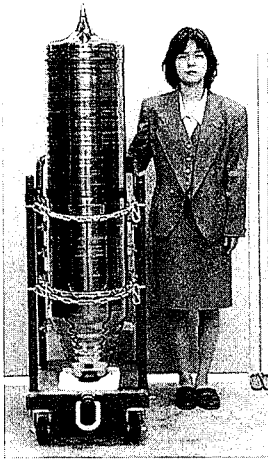
#### 4.2 Evaluation of crystal temperature gradient

Temperature inside the crystals was measured during the crystal growth with regards to the hot-zone in which the crystals were pulled. The temperature measurement was done on 300-mm diameter crystals with thermocouples embedded at the crystal center and 75 mm, 100 mm, 125 mm and 145 mm from the center (5 positions) after growing the crystals and cutting them into prescribed lengths. Fig. 3 shows radial position dependency of the temperature gradient in the crystal growth direction obtained through the crystal temperature measurement. The solid line is an approximation of the measurement data using a 4th order polynomial. With the hot-zone used in the tests, the temperature gradient differed by about 1.7 times between the center and the edge of the crystal.

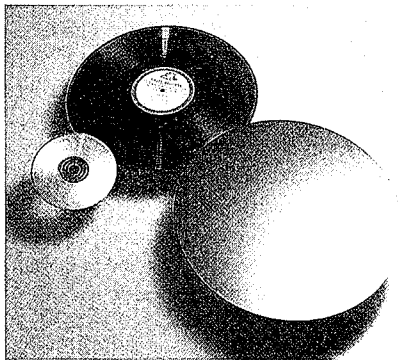
#### 4.3 Evaluation of ring OSF radius

Ring OSFs were made to appear by manufacturing wafers from the pulled-up crystals and heat-treating the wafers at 1,100°C for 1 h in a wet atmosphere for oxidation. Radiuses of the ring OSFs were obtained through X-ray topographic evaluation. Photo 2 is an X-ray topograph of a 300-mm diameter P<sup>+</sup> crystal.

Fig. 4 shows the relationship between the ring OSF radius and



(a) 300-mm diameter silicon single crystal



(b) 300-mm diameter silicon wafer

Photo 1

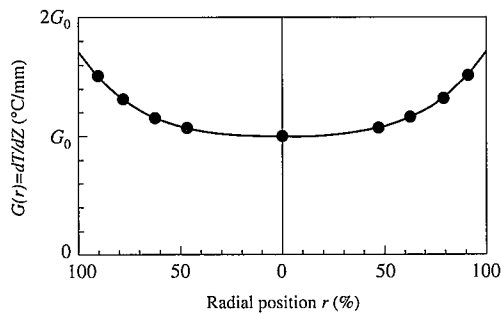


Fig. 3 Temperature gradient along crystal growth direction in relation to radial position during growth of 300-mm diameter crystal

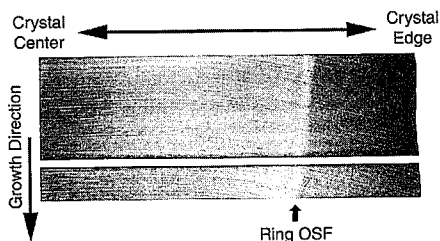


Photo 2 X-ray topograph of 300-mm diameter P+ crystal

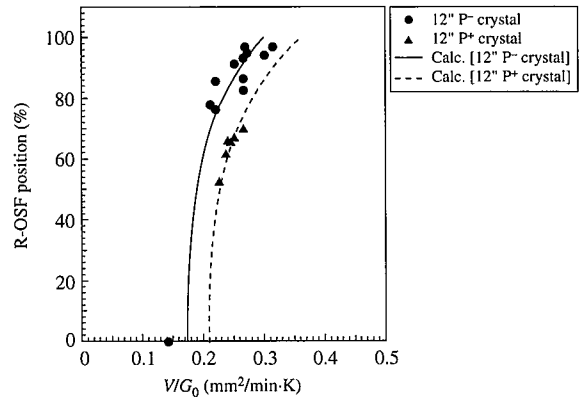


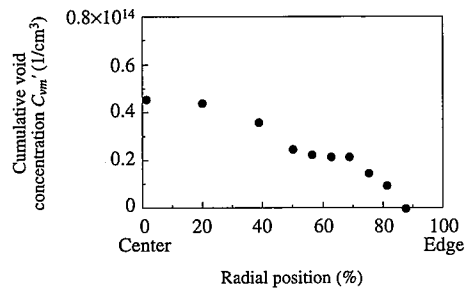
Fig. 4 Ring OSF radius in relation to  $V/G_0$  in 300-mm diameter crystal

the ratio  $V/G_0$  of the crystal growth rate  $V$  to the temperature gradient in the crystal growth direction at the center  $G_0$  of the crystals grown under different pulling rates. Since the temperature gradient in the crystal growth direction at the center  $G_0$  is constant, we see from the figure that, either in the P- crystals or the P+ crystals, the ring OSF moves from the center towards the crystal edge as the crystal growth rate  $V$  becomes larger.

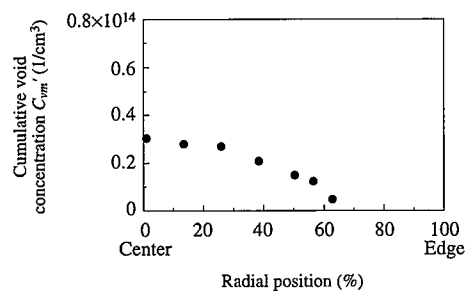
#### 4.4 Evaluation of void defects

Void defects of wafers were measured with an optical precipitate profiler (OPP) using as-grown wafers (without heat treatment) after polishing the wafers manufactured from the pulled-up crystals. Since the OPP is capable of measuring both the size and concentration of void defects, cumulative void concentration can be calculated from the OPP measurement results<sup>10</sup>.

Fig. 5 shows the cumulative void concentration of P- crystals and P+ crystals evaluated with the OPP. We see here that the nearer the wafer center the higher the cumulative void concentration becomes in either type of crystals. The position where the cumulative



(a) P- crystal



(b) P+ crystal

Fig. 5 Cumulative void concentration in relation to radial position during growth of 300-mm diameter crystal

void concentration becomes zero roughly coincides with the position of the ring OSF, and there are dislocation cluster defects in the wafer peripheral region where no void defects are found.

5. Discussions

5.1 Relationship between ring OSF and  $V/G(r)$

As shown in Fig. 3, the temperature gradient in the crystal growth direction is different in a crystal radial position and is determined by the hot-zone. The relationship between the ring OSF radius and  $V/G_0$  shown in Fig. 4, therefore, depends also on the hot-zone and not on the material characteristics of silicon only. Hence, to examine unique material characteristics of silicon independent from the hot-zone, it is necessary to compensate the temperature gradient in the crystal growth direction for its radial position dependency.

Fig. 6 shows the relationship of the ring OSF radius with  $V/G(r)$  of 300-mm diameter silicon crystals. The critical value  $(V/G)_{crit}$  for the ring OSF to appear at the crystal center is different in the P<sup>-</sup> crystals and the P<sup>+</sup> crystals, but the ring OSF is formed in either type of crystals at the position where the ratio  $V/G(r)$  of the crystal growth rate  $V$  to the temperature gradient in the crystal growth direction at a ring OSF radius  $r$   $G(r)$  becomes equal to the critical value  $(V/G)_{crit}$ . Thus it has been confirmed that distribution of the ring OSF is univocally determined by  $V/G(r)$ . The critical value  $(V/G)_{crit}$  for the ring OSF to appear is 0.17 mm<sup>2</sup>/min·°C for the P<sup>-</sup> crystals and is 0.21 mm<sup>2</sup>/min·°C for the P<sup>+</sup> crystals. These values are somewhat different in different reports<sup>7,11</sup>, but the difference can be attributed to inaccurate measurement of the temperature gradient in the crystal growth direction, and further investigations are required to clarify this issue.

The solid line in Fig. 4 shows the ring OSF radius in relation to  $V/G_0$ , the ring OSF radius being calculated from the critical value  $(V/G)_{crit}$  for each of the crystals and from  $G(r)$ , and is in good agreement with the measurement data, like Fig. 6.

5.2 Effects of boron addition on grown-in defects

Since radial distribution of the cumulative void concentration shown in Fig. 5 is dependent on the hot-zone like in the case of the ring OSF analysis, we re-plotted the cumulative void concentration in relation to  $V/G(r)$  for the purpose of eliminating the effects of the hot-zone (see Fig. 7). The value of  $V/G(r)$  where the cumulative void concentration is equal to zero is very close to  $(V/G)_{crit}$  either in the P<sup>-</sup> crystals or the P<sup>+</sup> crystals.

Several models have been proposed as grown-in defect forming models<sup>12,13</sup> such as the Voronkov model<sup>14</sup>, the Habu model<sup>15</sup>, etc. The test results were examined using the Voronkov model, one of the simplest among the proposed models.

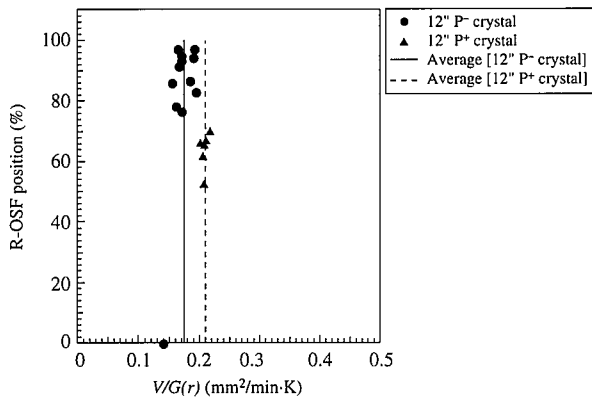


Fig. 6 Ring OSF radius in relation to  $V/G(r)$  in 300-mm diameter crystal

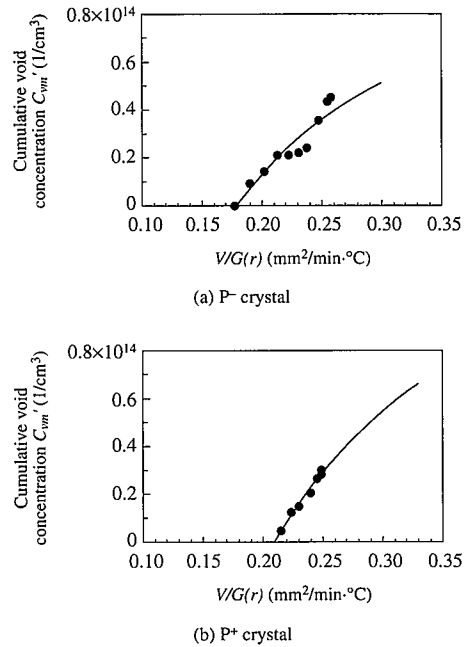


Fig. 7 Cumulative void concentration in relation to  $V/G(r)$  in 300-mm diameter crystal

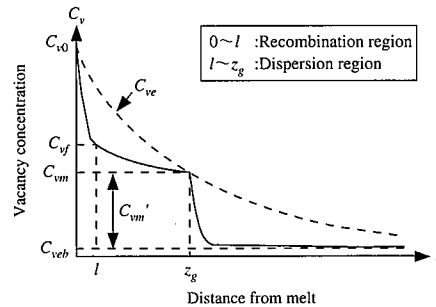


Fig. 8 Voronkov model (case of excessive vacancy)

Thus, the model assumes the following two hypotheses regarding the crystal growth from a silicon melt (see Fig. 8):

- (1) Vacancies and interstitial atoms are introduced to the crystal during solidification of the melt in the quantities corresponding to their respective equilibrium concentrations at the melting temperature.
- (2) The vacancies and interstitial atoms disappear in pairs within several millimeters of liquid/solid boundary.

Because the vacancies and interstitial atoms flow into the crystal in proportion to the concentration gradient in the crystal, the flux  $J$  of vacancies in the case of excessive vacancies is expressed as follows:

$$J = \left( VC_v - D_v \frac{\partial C_v}{\partial z} \right) - \left( VC_i - D_i \frac{\partial C_i}{\partial z} \right) \quad (1)$$

where  $V$  is crystal growth rate,  $C_v$  is concentration of vacancies,  $C_i$  is concentration of interstitial atoms,  $D_v$  is mobility of vacancies in the crystal,  $D_i$  is mobility of interstitial atoms in the crystal, and  $z$  is position in the crystal growth direction from melt surface. When the value of  $J$  is negative, it should be interpreted as the flux of interstitial atoms.

Vacancies become dominant and void defects appear when the

crystal growth rate is high, whereas interstitial atoms become dominant and dislocation cluster defects appear when the crystal growth rate is low. From this and the above two assumptions it is considered that concentration of the vacancies introduced to the crystals at the initial stage  $C_{v0}$  is larger than the concentration of interstitial atoms  $C_{i0}$  ( $C_{v0} > C_{i0}$ ), and that  $D_v C_{v0}$  is smaller than  $D_i C_{i0}$  ( $D_v C_{v0} < D_i C_{i0}$ ).

A linear approximation of crystal temperature near the solid/liquid boundary in relation to the position along the crystal growth direction makes it possible to express the equilibrium concentrations of vacancies  $C_{ve}$  and interstitial atoms  $C_{ie}$  in terms of their respective formation energies  $E_v$  and  $E_i$  as follows:

$$C_{ve} = C_{v0} e^{-\frac{E_v G Z}{k T_0^2}}, C_{ie} = C_{i0} e^{-\frac{E_i G Z}{k T_0^2}} \quad (2)$$

where  $T_0$  is crystal temperature at the solid/liquid boundary, and  $G$  is crystal temperature gradient at the same boundary. It so follows that the critical concentration of vacancies  $C_{vm}$  for them to phase-transform into void defects by aggregation can be approximated as follows<sup>16)</sup>:

$$C_{vm} (V/G(r)) = \frac{J}{V} = (C_{v0} - C_{i0}) \left( 1 - \frac{(V/G)_{crit}}{V/G(r)} \right) \quad (3)$$

It has to be noted here that Eq. (3) was obtained through extension of a 1-dimensional model into a 2-dimensional model in which extension the temperature gradient in the crystal growth direction  $G$  assumed to be homogeneous in a crystal section in the 1-dimensional model was replaced with a temperature gradient in the crystal growth direction  $G(r)$  having a radial position dependency.

On the other hand, the cumulative void concentration  $C_{vm}'$  measured with the OPP is the difference between  $C_{vm}$  and equilibrium vacancy concentration at room temperature  $C_{veb}$  ( $C_{vm}' = C_{vm} - C_{veb}$ ). Since  $C_{vm}' \sim 10^{14} (1/cm^3)$  is true from the measurement results and  $C_{veb} \sim 10^{12} (1/cm^3)$  is also true<sup>17)</sup>, it follows that  $C_{vm} \doteq C_{vm}' \gg C_{veb}$  holds true. Consequently, Eq. (3) is further approximated as follows:

$$C_{vm}' (V/G(r)) = C_{vf} \cdot \left( 1 - \frac{(V/G)_{crit}}{V/G(r)} \right) \quad (4)$$

where  $C_{vf}$  is initial excessive vacancy concentration, that is asymptotic cumulative void concentration, after the pair annihilation of primary defects and is equal to  $C_{v0} - C_{i0}$ .

The cumulative void concentration was fitted in relation to  $V/G(r)$  using Eq. (4) with  $C_{vf}$  and  $(V/G)_{crit}$  as parameters. The result is shown in the solid line in Fig. 7. The asymptotic cumulative void concentration  $C_{vf}$  obtained through the fitting is  $1.3 \times 10^{14} (1/cm^3)$  for the P- crystals and  $1.8 \times 10^{14} (1/cm^3)$  for the P+ crystals. Fig. 9 shows the asymptotic cumulative void concentration  $C_{vf}$  in relation to boron concentration. We understand from the figure that the asymptotic cumulative void concentration does not change with increase in the boron concentration, or that it increases only slightly.

The critical value  $(V/G)_{crit}$  of  $V/G$  for the ring OSF to appear is expressed as follows<sup>12)</sup>:

$$\left( \frac{V}{G} \right)_{crit} = \frac{E_i + E_v}{2k_0 T_0^2} \cdot \frac{D_i C_{i0} - D_v C_{v0}}{C_{v0} - C_{i0}} = \frac{E_i + E_v}{2k_0 T_0^2} \cdot \frac{D_i C_{i0} - D_v C_{v0}}{C_{vf}} \quad (5)$$

On an assumption that  $T_0$ ,  $E_v$  and  $E_i$  do not change, from Eq. (5), the critical value  $(V/G)_{crit}$  may increase with an increase in the boron concentration in the following three hypothetical cases:

- (1) Where the mobility of vacancies  $D_v$  decreases or the mobility of interstitial atoms  $D_i$  increases.
- (2) Where  $C_{vf} (= C_{v0} - C_{i0})$  decreases.
- (3) Where concentrations of vacancies and interstitial atoms  $C_{v0}$  and

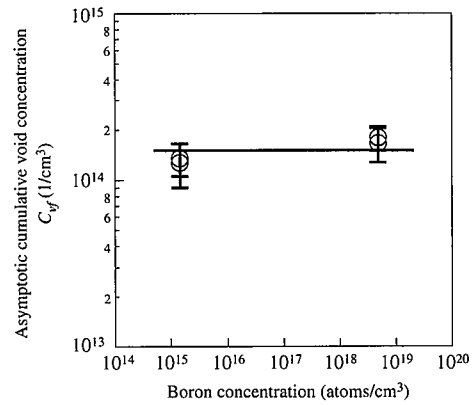


Fig. 9 Asymptotic cumulative void concentration in relation to boron concentration

$C_{i0}$  increase under the condition that  $C_{vf} (= C_{v0} - C_{i0})$  is constant. Among the above, however, (2) contradicts the test result. With regards to (3), although there is a report to the effect that interstitial atoms increase with boron addition by the size effect of boron atoms<sup>9)</sup>, it is not plausible that two types of defects opposite in nature to each other should increase simultaneously, keeping the difference between them. Thus, as a conclusion, (1) is the most likely. Susanto et al. explained that boron formed pairs with vacancies or interstitial atoms and that, with increasing boron concentration, the radius of the ring OSF came inside the crystal because of low mobility of the pairs<sup>8)</sup>. This supports (1) above.

Changes in mobility of the species based on the test results were also estimated. On an assumption that the mobility of interstitial atoms  $D_i$  stays constant and only that of vacancies  $D_v$  changes, the mobility of vacancies of a P+ crystal  $D_v^+$  is expressed as follows:

$$\frac{D_v^+}{D_v} = \frac{(V/G)_{crit}^+}{(V/G)_{crit}} \left( 1 - \frac{C_{i0}}{C_{v0}} \cdot \frac{D_i}{D_v} \right) + \frac{C_{i0}}{C_{v0}} \cdot \frac{D_i}{D_v} \quad (6)$$

where  $(V/G)_{crit}^+$  is the critical value  $(V/G)_{crit}$  of a P+ crystal. The mobility will decrease by about 5 to 18%, when  $C_{v0}/C_{i0} = 1.07$  and  $D_i/D_v = 0.71$  are applied to the equation<sup>14)</sup>. The difference in the mobility decrease (or the above value not being univocally determined) is attributed to whether to consider the asymptotic cumulative void concentration  $C_{vf} (= C_{v0} - C_{i0})$  to be constant independent from boron concentration or it increases as the boron concentration increases. It is thought however, that the measurement result does not have the accuracy for examining the difference, since it consists only of the data obtained with an OPP and the value of the asymptotic cumulative void concentration was estimated from the measurement data obtained where the cumulative void concentration was small. This issue has to be studied in the future.

## 6. Conclusion

It has been confirmed through tests using 300-mm diameter CZ-Si crystals that ring OSFs generating to the crystals would become manifest when the ratio  $V/G(r)$  of the crystal growth rate  $V$  to the temperature gradient in the crystal growth direction  $G(r)$  becomes equal to a critical value  $(V/G)_{crit}$ . This holds true with either the P- crystals or the P+ crystals, although the critical value  $(V/G)_{crit}$  becomes larger as boron concentration increases. For controlling the ring OSF it is important to control radial distribution of the temperature gradient in the crystal growth direction, and for this end, design technology of the hot-zone of pulling furnaces will play a key role.

The cumulative void concentration in the CZ-Si crystals can be expressed in the form of equation using  $V/G(r)$  as a parameter. It was learned that the concentration of excessive vacancies  $C_v$  introduced to a crystal was in the same order of magnitude in the P<sup>-</sup> crystals and the P<sup>+</sup> crystals. From this it can be concluded that the increase in the critical value  $(V/G)_{crit}$  caused by an increase in boron concentration is accounted for with effective decrease in the mobility of vacancies, etc. when a simplified Voronkov model is assumed.

Application of these findings to the quality design of the silicon crystals will make quality enhancement viable in parallel to the diameter expansion of the crystals.

#### Reference

- 1) Ryuta, J., Morita, E., Tanaka, T., Shimanuki, Y. : Jpn. J. Appl. Phys. 29, L1947 (1990)
- 2) Takeno, H., Ushio, S., Takenaka, T. : Mat. Res. Symp. Proc. 262, 51 (1992)
- 3) Hasebe, M., Takeoka, Y., Shinoyama, S., Naito, S. : Jpn. J. Appl. Phys. 26, L1999(1989)
- 4) Hourai, M., Nagashima, T., Kajita, E., Miki, S., Shigematsu, T., Okui, M. : J. Electrochem. Soc. 142, 3193 (1995)
- 5) Ammon, W.V., Dornberger, E., Oelkrug, H., Weidner, H. : J. Crystal Growth 151, 273 (1995)
- 6) Voronkov, V.V. : Report at JSPS Symposium, Tokyo, 1997-11-28
- 7) Dornberger, E., Ammon, W.V. : J. Electrochem. Soc. 143, 1636 (1996)
- 8) Susanto, Hendi : Electrochemical Society Proceedings. Vol.99-1, p.479-490
- 9) Kikuti, M. et al.: The 60th Meeting Extended Abstracts 2a-S-10, Vol.1, The Japan Society of Applied Physics, 1999, p.349
- 10) Nakai, K., Hasebe, M., Iwasaki, T., Tsumori, Y. : Mat. Res. Soc. Symp. Proc. Vol.1, 1997, p.442
- 11) Nakamura, H. et al.: The 47th Meeting Extended Abstracts 30a-YM-2, Vol.1, Japan Society of Applied Physics, 2000, p.426
- 12) Tan, T.Y., Goesele, U. : Appl. Phys. A37, 1(1985)
- 13) Brown, R., Maroudas, D., Sinno, T. : J. Crystal Growth 137, 12(1994)
- 14) Voronkov, V.V. : J. Crystal Growth. 59, 625 (1982)
- 15) Habu, R., Tomiura, A., Harada, H. : Semicond. Silicon, ECS, Pennington N.J., 1994, p.635
- 16) Voronkov, V.V., Falster, R. : J. Crystal Growth. 194, 76(1998)
- 17) Zulehner, W. : Springer Series in Mat. Sci. Vol 13, Semicond. Silicon. Ed. G. C. Harbeke, M. J. Schulz, 1989